Clinical Biomechanics 49 (2017) 119–127

Contents lists available at ScienceDirect

Clinical Biomechanics

journal homepage: www.elsevier.com/locate/clinbiomech

Lecture

In vivo biomechanical behavior of the trapeziometacarpal joint in healthy and osteoarthritic subjects☆

Priscilla D'Agostino[a,b,c,*,1], Benjamin Dourthe[a,1], Faes Kerkhof[a], G. Harry Van Lenthe[d], Filip Stockmans[a,e], Evie E. Vereecke[a]

[a] Muscles & Movement, Department of Development and Regeneration, Biomedical Sciences Group, KU Leuven Campus Kulak, Kortrijk, Belgium
[b] Louise Hand Clinic, Brussels, Belgium
[c] Europe Clinic, St-Elisabeth Clinic, Brussels, Belgium
[d] Biomechanics Section, Science, Engineering & Technology Group, KU Leuven, Leuven, Belgium
[e] Handgroep, AZ Groeninge, Kortrijk, Belgium

ARTICLE INFO

Keywords:
Thumb
TMC joint
In vivo contact biomechanics
Osteoarthritis

ABSTRACT

Background: The contact biomechanics of the trapeziometacarpal joint have been investigated in several studies. However, these led to conflicting results and were mostly performed in vitro. The purpose of this study was to provide further insight on the contact biomechanics of the trapeziometacarpal joint by in vivo assessment of healthy and osteoarthritic subjects.

Methods: The hands of 16 healthy women and 6 women with trapeziometacarpal osteoarthritis were scanned in positions of maximal thumb extension, flexion, abduction and adduction during three isometric tasks (lateral key pinch, power grasp and jar twist) and in thumb rest posture (relaxed neutral). Three-dimensional surface models of the trapezium and first metacarpal were created for each thumb configuration. The articular surface of each bone was measured in the neutral posture. A computed tomography-based proximity mapping algorithm was developed to calculate the distance between opposing joint surfaces, which was used as a surrogate for intra-articular stress.

Findings: Distinct proximity patterns were observed across tasks with a recurrent pattern reported on the volar aspect of the first metacarpal. The comparison between healthy and arthritic subjects showed a significantly larger articular area, in parallel with a significant joint space narrowing and an increase in proximity area in arthritic subjects. We also observed severe articular deformations in subjects with late stage osteoarthritis.

Interpretation: This study has increased our insight in the contact biomechanics of the trapeziometacarpal joint during tasks and positions of daily life in healthy and arthritic subjects, which might contribute to a better understanding of the occurrence mechanisms of degenerative diseases such as osteoarthritis.

1. Introduction

The trapeziometacarpal (TMC) joint has a highly important role in human thumb function (Neumann and Bielefeld, 2003). Its concavo-convex structure allows thumb opposition and provides the human hand with advanced prehension abilities (Edmunds, 2011; Koff et al., 2003; Tsai and Beredjiklian, 2008). The high mobility of the TMC joint makes it also prone to osteoarthritis (OA), a very common multi-factorial degenerative joint disorder. Due to the highly disabling symptoms of TMC OA and its large impact on hand function, the TMC

☆ **Author contributions:**
PDA made contributions to the study design, was responsible for participant recruitment, data collection, data processing, analysis and interpretation, drafting, editing and revising the manuscript, and contributed to the figures creation.
BD made contributions to the study design, was responsible for data processing, analysis and interpretation, drafting, editing and revising the manuscript and for creation of the figures.
FK made contributions to the analysis and interpretation of the data.
HVL made contributions to data interpretation, editing and revising the manuscript.
FS made contributions to the conception and design of the study, to participant recruitment and interpretation of the data.
EEV made contributions to the study concept and design, to participant recruitment, data analysis and interpretation, editing and revising the manuscript.
All authors have read and approved the final submitted manuscript.

* Corresponding author at: Louise Hand Clinic, Avenue Louise, 284, B-1050 Brussels, Belgium.
E-mail address: priscilla.dagostino@kuleuven.be (P. D'Agostino).
[1] These authors contributed equally to this work.

http://dx.doi.org/10.1016/j.clinbiomech.2017.09.006
Received 3 June 2017; Accepted 11 September 2017

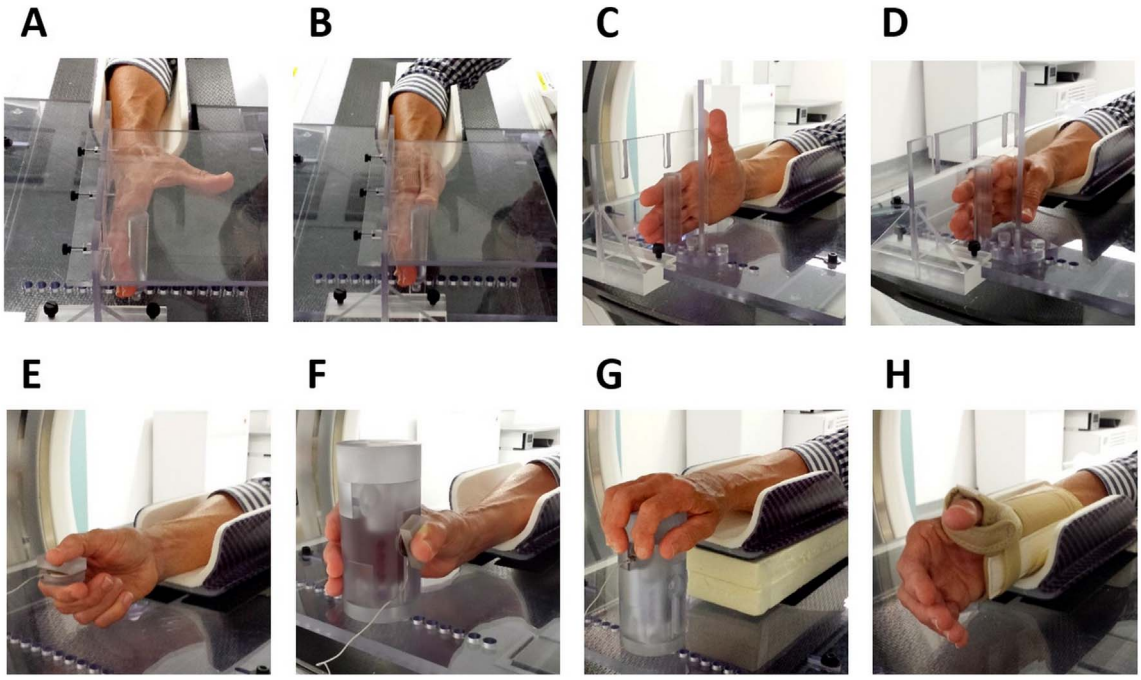

Fig. 1. Photos showing the different scanning configurations: A: maximal abduction, B: maximal adduction, C: maximal extension, D: maximal flexion, E: lateral key pinch, F: power grasp, G: jar twist, H: relaxed neutral.

joint has been reported as the most common site for surgical reconstruction in the hand (Batra and Kanvinde, 2007; Nicholas and Calderwood, 1992).

Several factors have been correlated with the development of OA, including systemic susceptibilities and mechanical factors. Genetic inheritance, hormonal variations, excessive and/or unusual joint loading, ligament laxity, muscular weaknesses and variations in articular morphology all represent potential OA prevalence factors (Brandt et al., 2009; Felson, 2000; Fontana et al., 2007; Hunter and Wilson, 2009; Wilson et al., 2008). The lack of joint congruence (i.e. geometric correspondence between two opposing articular surfaces), has also been associated with TMC OA development due to the higher risk of intra-articular peak pressures in incongruent joints (Ateshian et al., 1992; Pelligrini, 1991a; Wilson et al., 2013). This conclusion was recently discussed by Conconi et al. (2014).

Many in vitro studies have been performed to understand the contact biomechanics of the TMC joint (Ateshian et al., 1995; Cheema et al., 2012; Koff et al., 2003; Kovler et al., 2004; Momose et al., 1999; Moulton et al., 2001; Pellegrini et al., 1993; Pelligrini, 1991b), with strong inconsistencies between results. These investigations were also limited by the invasiveness of their methodologies, which are not applicable in vivo (e.g. casting methods, pressure-sensitive film). To our knowledge, only a few recent studies have assessed the levels of joint congruence in healthy and arthritic TMC joints in vivo (Conconi et al., 2014; Dourthe et al., 2016; Goto et al., 2014; Halilaj et al., 2014a, 2015).

We developed a medical image-base protocol to assess the differences in TMC joint proximity patterns between healthy and arthritic subjects, with proximity area as a surrogate for joint congruence. We hypothesize that proximity area and pattern will differ between thumb postures, with a volar predominance on the articular facet of the first metacarpal (MC1), in agreement with the location of cartilage eburnation sites reported in patients with late stage TMC OA (Koff et al., 2003; Pellegrini et al., 1993; Pelligrini, 1991b; Xu et al., 1998). We also expect to observe a significant joint space narrowing and enlargement of the articular surfaces in patients with TMC OA (Halilaj et al., 2014b, 2015).

2. Methods

2.1. Subject selection

After permission by the Medical Ethical Commission of the University of Leuven (Belgium, # B322201420166), 22 female volunteers (mean age: 60.1 years, range: 50–82 years, 17 right and 5 left dominant hand) were recruited among the staff of the university and through medical consultations (FS) at the hospital AZ Groeninge (Kortrijk, Belgium). Considering the high incidence of TMC OA in postmenopausal women (Wilder et al., 2006), and to avoid any age- or sex-related statistical impact on the results, only female volunteers of 50 years or more were recruited. Exclusion criteria included several comorbidities such as thumb traumatic injury/surgery, inflammatory arthritis and metabolic bone disease. Each subject signed an informed consent and completed the Disabilities of Arm, Shoulder and Hand questionnaire (DASH) and the Patient Rated Wrist Evaluation questionnaire (PRWE). Both hands were examined by an orthopaedic hand surgeon (PDA) to determine the dominant hand and assess the radiological stage of TMC OA (Eaton et al., 1984; Eaton and Glickel, 1987). The dominant hand was defined as the hand showing the greatest strength during lateral pinch and power grasp.

2.2. Subject classification

Volunteers were classified in two groups: the healthy group (n = 16, mean age: 59.5 years, range: 50–82 years) included asymptomatic subjects with no radiological signs of OA and low DASH and PRWE scores (mean DASH: 3.9 (standard deviation (SD): 4.5); mean PRWE: 1.5 (SD: 2.4)), while the OA group (n = 6, mean age: 61.8 years, range: 51–71 years) was composed of symptomatic subjects with Eaton stage = III-IV and high DASH and PRWE scores (mean DASH: 34.2 (SD: 20.2); mean PRWE: 42.0 (SD: 27.4)).

2.3. Scanning protocol

Each dominant (healthy group) or affected (OA group) hand was scanned from the distal part of the radius to the first

metacarpophalangeal joint in eight different configurations using a 64 slice Discovery HD 750 CT scanner (slice thickness: 0.625 mm, pixel size: 0.293 mm, 100 kV, 156 mA, GE Healthcare, Little Chalfont, UK) at the hospital AZ Groeninge (Kortrijk, Belgium).

Four static CT scans were taken in different thumb postures using a radiolucent jig (Crisco et al., 2015a, 2015b): maximal abduction (ABD), maximal adduction (ADD), maximal extension (EXT) and maximal flexion (FLEX) (Fig. 1A–D). Three additional loaded scans were taken while performing lateral key pinch (KPINCH), power grasp (GRASP) and jar twist (JAR) (Fig. 1E–G) using the same jig with an embedded compression load cell (0–50 lb [0–22.7 kg]; Model D Thu-Hole Load Cell; Honeywell International Inc., Morristown, NJ, USA) (Halilaj et al., 2014c; Luker et al., 2014). These scans were taken at a sub-maximal force corresponding to 80% of the subject's maximal strength for the specific task. This relative value was chosen instead of a constant absolute target value to allow comparison between subjects without accounting for differences in strength abilities. In addition, OA patients might not have been able to reach a specific targeted force due to the advanced symptoms. For each subject and for each task, the maximal force was measured prior to CT scanning. During data acquisition, each subject was able to execute the tasks at a constant sub-maximal force, which was monitored by giving live visual feedback of the applied force. To limit muscular fatigue, we asked each subject to start applying force only a few seconds before initializing the acquisition and acquisition time was limited to 5–10 s. Every subject was easily able to maintain a constant submaximal force without any complaints of fatigue. Lastly, a static CT scan was taken in a relaxed neutral posture (NEUT) using a thumb splint (Rolyan®Original; Patterson Medical, Bolingbrook, IL, USA) (Fig. 1H).

2.4. Image segmentation

Each scan was reconstructed in a DICOM format and segmented semi-automatically using medical imaging processing software (Mimics Research 18.0 × 64 with CT bone plug-in, Materialise, Leuven, Belgium) with constant segmentation parameters (thresholding: min. of 294 Hounsfield, smoothing: 1 iteration, smooth factor of 0.4). Three-dimensional (3D) surface meshes of the MC1 and the trapezium were generated with an average edge length of < 0.5 mm.

2.5. Articular area

The **articular area** of each bone was measured manually in the neutral configuration with an anatomical CAD software (3-matic Research 10.0 × 64, Materialise, Leuven, Belgium) by following the visible junction between the bony contour and the limit of the articular cartilage (Fig. 2A). Two observers (PDA and BD) performed a series of five measurements on each 3D bone model (i.e. MC1 and trapezium; 22 subjects) to assess the repeatability of the method. The average of the ten corresponding measurements (assessed by both observers) was reported as the average articular area.

2.6. Joint proximity

We developed an approach based on joint proximity, which can be considered as a surrogate for stress distribution assessment (Goto et al., 2014). We designed a custom-written code in Matlab (v. R2014a × 64, MathWorks, Inc.) which calculates the Euclidean distances between points located on the subchondral surface of the proximal articular facet of the MC1 and the distal articular facet of the trapezium within a 3 mm range (Goto et al., 2014). The **minimal joint space** was defined as the minimal distance calculated for the two closest vertices of each bone. The results were displayed as proximity maps on the articular surface of each 3D bone model based on a custom color scale (Fig. 2B).

To assess the level of joint congruence, a normal physiological joint space of 1.5 mm was defined based on the combined thicknesses of healthy MC1 and trapezial cartilage layers (Koff et al., 2003). Each set of points (i.e., two closest neighbors on the MC1 and trapezium) for which the joint space was below this threshold was considered within the **proximity area** (in red, Fig. 2B). To aid visual interpretation of the proximity maps, nine sub-regions were defined. Two principal axes (dorsal-volar and radial-ulnar) were determined based on anatomical landmarks (Fig. 3). These two axes were divided in three equal segments which defined the corresponding nine sub-regions (Dourthe et al., 2016). Based on this articular sub-division, the location of the proximity area was categorically defined for each configuration and all subjects ('**proximity pattern**').

2.7. Joint curvature

For each subject, the **curvatures** of the articular facets of the MC1 and trapezium were calculated along the dorsal-volar and radial-ulnar axes in the neutral configuration. A custom-written code was designed in Matlab to screen the articular surfaces of each bone along both directions by creating cross-sectional frames (n = 50). Each group of points (n ≥ 3) located within one frame was used to calculate the best circle fit. The local curvature was then calculated as the inverse of the radius of the corresponding circle. The average of each local curvature was computed to represent the mean articular curvature along each axis.

2.8. Statistical analysis

Normality of the data was ensured using a Shapiro-Wilk test. The differences between groups (healthy vs. OA) and between bones (MC1 vs. trapezium) were tested with a Student *t*-test (Welch two sample *t*-test, one- or two-sided, unequal variances). These *t*-tests were used for the parameters articular area, proximity area, minimal joint space and curvature. In addition, a *t*-test was also used to compare between dorsal-volar and radial-ulnar curvatures. ANOVAs were used to test the effect of thumb posture (fixed effect) and subject (random effect) and to include interaction effects in the model design for the parameters minimal joint space and proximity area.

The interrater reliability for measuring the articular area was evaluated using Kendall's coefficient of concordance. There was a high agreement between the measurements of both raters ($W = 0.977$, $t = 426$, $P < 0.0001$). The repeatability of the area measurement was quantified using the intraclass correlation coefficient (ICC, 5 measurements per bone per subject). The ICC was high for each observer (ICC > 0.96). The high consistency both between and within observers supports the averaging of articular area over all measurements taken per sample (5 measurements × 2 observers).

All statistical tests were calculated using R ("R Core Team. R: A language and environment for statistical computing", 2013). A *P*-value of < 0.05 was considered as statistically significant.

3. Results

3.1. Articular area

The articular areas measured for the OA group were significantly larger than for the healthy group, with an increase of > 100% for both the MC1 (135 mm^2 to 283 mm^2; $t = -14.98$, $df = 42$, $P < 0.0001$) and the trapezium (128 mm^2 to 267 mm^2; $t = -22.63$, $df = 63$, $P < 0.0001$). In the healthy group, the articular area of the MC1 (135 mm^2 (SD: 11 mm^2)) was significantly larger than that of the trapezium (128 mm^2 (SD: 14 mm^2) $t = 3.45$, $df = 148.02$, $P < 0.001$). In the OA group, this difference was not significant between bones ($t = 1.25$, $df = 57.10$, $P = 0.22$) but there was a higher inter-individual variation (SD > 50 mm^2).

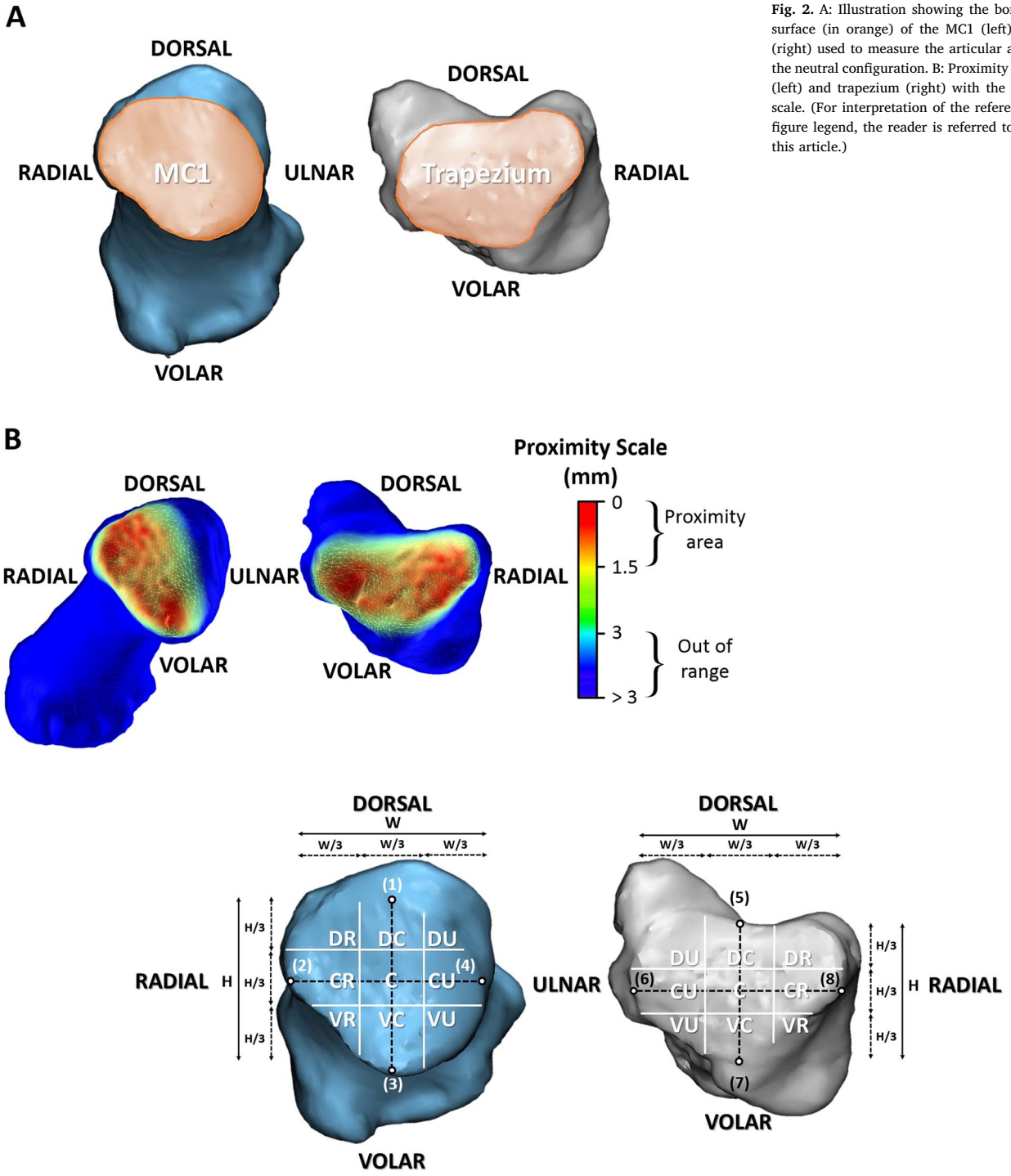

Fig. 2. A: Illustration showing the border of the articular surface (in orange) of the MC1 (left) and the trapezium (right) used to measure the articular area of each bone in the neutral configuration. B: Proximity mapping of the MC1 (left) and trapezium (right) with the corresponding color scale. (For interpretation of the references to color in this figure legend, the reader is referred to the web version of this article.)

Fig. 3. Articular area sub-division model used for the MC1 (left) and trapezium (right). Two bony landmarks were selected to define the dorsal-volar axis of the MC1: the highest point on the dorsal edge of the subchondral surface (1) and the highest point of the palmar beak (3). The dorsal-volar axis of the trapezium was defined based on: the lowest point on the dorsal border of the subchondral surface (5) and the lowest point of the volar edge (7). The radial-ulnar axis was defined as the line perpendicular to the dorsal-volar axis which passes through its center. This axis connects the two lowest points of the radial (2) and ulnar (4) aspects of the MC1, and the radial (6) and ulnar (8) horns of the trapezium. With: W: width, H: height, DR: dorsal-radial, DC: dorsal-central, DU: dorsal-ulnar, CR: central-radial, C: central, CU: central-ulnar, VR: volar-radial, VC: volar-central, VU: volar-ulnar.

3.2. Minimal joint space and proximity area

In the healthy group, the minimal joint space was slightly higher during the neutral, adduction, extension and lateral key pinch configurations than during the abduction, flexion, power grasp and jar twist configurations (range: 0.58 mm during power grasp to 0.86 mm in the neutral configuration). In the OA group, the minimal joint space was close to zero in every configuration, as expected based on the phenomenon of joint space narrowing observed in patients with degenerative OA (Eaton et al., 1984; Eaton and Glickel, 1987).

The proximity areas calculated in the OA group were significantly larger than in the healthy group (Fig. 4), both for the MC1 (190.3 mm^2 vs. 58.5 mm^2; t = 10.8, df = 48.9, $P < 0.0001$) and trapezium (188.3 mm^2 vs. 58.6 mm^2; t = −11.7, df = 49.2, $P < 0.0001$). In both groups there was no significant difference between the proximity areas of the MC1 and trapezium (healthy: t = −0.02, df = 251.9,

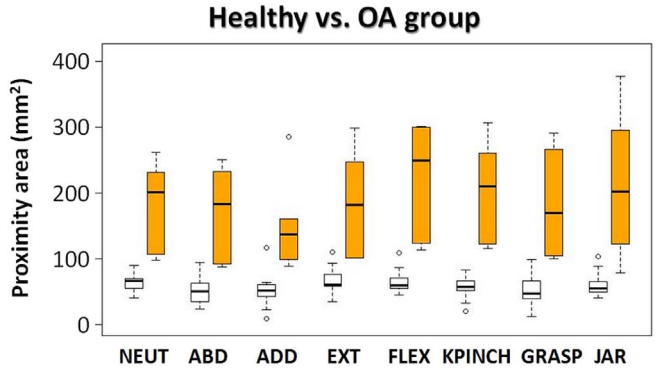

Fig. 4. Box plots representing the average proximity areas (MC1 + trapezium) calculated for each configuration in both groups (white: healthy – orange: OA). (For interpretation of the references to color in this figure legend, the reader is referred to the web version of this article.)

$P = 0.98$; OA: t = 0.1, df = 93.2, $P = 0.5$). The healthy group displayed a smaller proximity area during extension compared with abduction ($P < 0.0001$), flexion ($P < 0.005$) and lateral key pinch ($P < 0.05$), taking into account the effect of subject ($P < 0.0001$). In the OA group, the proximity area was also smallest during extension (significant compared to JAR: $P < 0.05$ and KPINCH: $P < 0.05$) and there was no significant effect of subject (F = 0.93, df = 8–87, $P = 0.5$).

3.3. Proximity patterns

In the healthy group, we observed task-dependent proximity patterns (Fig. 5). The dorsal-radial, central-radial, volar-radial and volar-central sub-regions were the most recurrent patterns observed for the MC1, while the dorsal-radial, central, volar-radial, volar-central and volar-ulnar sub-regions were the most recurrent proximity patterns for the trapezium.

A proximity area shift from radial to volar-ulnar was observed between abduction and adduction, and between neutral and lateral key pinch, but only for the MC1. Conversely, between extension and flexion, a proximity area shift from dorsal-radial to volar-ulnar was observed, but only for the trapezium.

In the adduction, flexion and lateral key pinch configurations, the respective proximity areas of the MC1 and trapezium were not directly facing (e.g. adduction: central-volar for the MC1 and radial-volar for the trapezium).

In the OA group, proximity areas covered a large portion of the articular surface of the MC1 and trapezium and showed no difference between configurations.

3.4. Joint curvature

In the healthy group, the proximal facet of the MC1 was significantly more curved along the convex radial-ulnar axis than along the concave dorsal-volar axis (t = 9.21, df = 25.69, $P < 0.0001$). For the distal facet of the trapezium, the curvature was significantly stronger along the convex dorsal-volar axis than along the concave radial-ulnar axis (t = 9.04, df = 20.97, $P < 0.0001$) (Fig. 6A). The curvatures of the facets of the MC1 and trapezium were significantly different when comparing along both axes (dorsal-volar: t = −16.76, df = 29.739, $P < 0.00001$; radial-ulnar: t = 5.5933, df = 28.221, $P < 0.00001$) (Table 1).

In the OA group, we observed a significant flattening of the dorsal-volar convexity of the distal facet of the trapezium compared to the healthy group (t = 4.35, df = 6.52, $P < 0.01$) (Fig. 6B). We also observed a lengthening of the palmar beak of the proximal facet of the MC1 with a significant inversion of the curvature along the dorsal-volar axis (concave to convex; t = −2.40, df = 6.80, $P < 0.05$). The

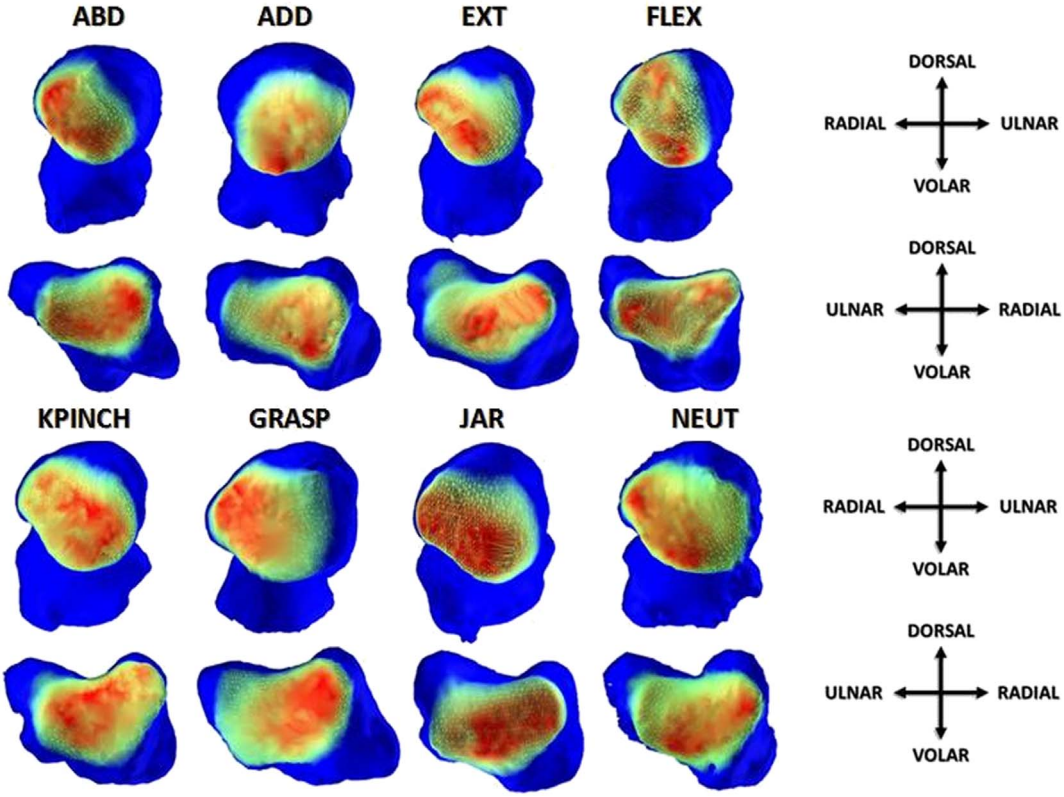

Fig. 5. 3D bone models representing the dominant proximity patterns (selected among subjects for being the most representative) observed on the articular surface of each bone for each configuration in the healthy group.

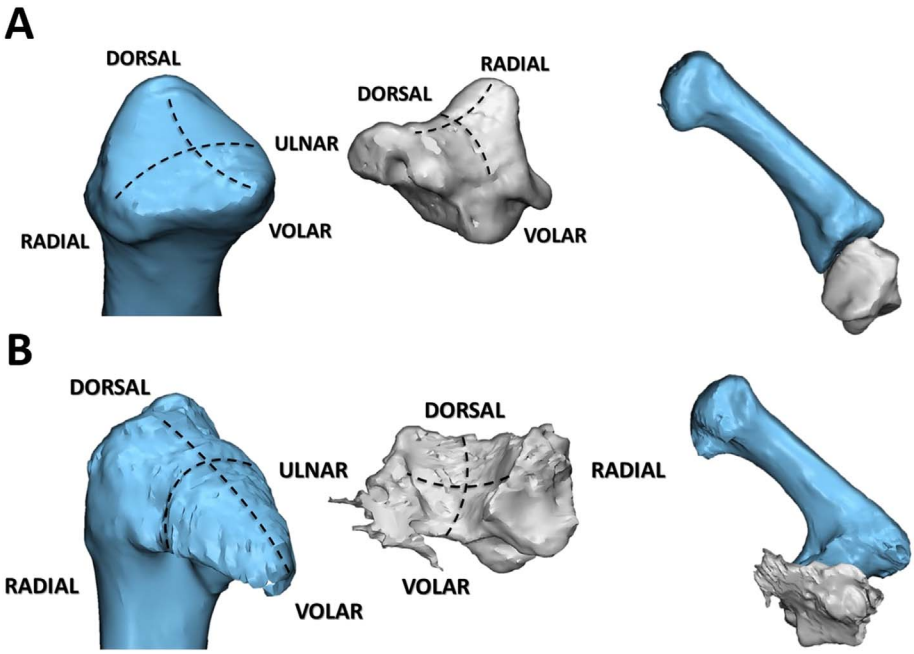

Fig. 6. 3D bone models of the MC1 (left, blue) and trapezium (middle, grey) representing the average dorsal-volar and radial-ulnar curvatures measured in the healthy (A) and OA (B) groups. A radial view of the corresponding TMC joint is also represented for both groups (right). (For interpretation of the references to color in this figure legend, the reader is referred to the web version of this article.)

Table 1
Mean curvatures (SD: standard deviation) calculated along the dorsal-volar and radial-ulnar axes of the MC1 and trapezium in each group. Note: a positive sign indicates a convex curvature and a negative sign indicates a concave curvature. Statistical significance of the P-values (i.e. *: $P < 0.05$; **: $P < 0.01$; ***: $P < 0.001$).

		Curvature healthy (mm^{-1})	Curvature OA (mm^{-1})	*t*-Test (group 1–2)
Dorsal-Volar	MC1	−0.03 (SD 0.03)	0.02 (SD 0.05)	0.049*
	Trapezium	0.16 (SD 0.03)	0.06 (SD 0.05)	0.004**
	T-test (MC1-Trap)	2.20×10^{-16}***	0.15	/
Radial-Ulnar	MC1	0.11 (SD 0.05)	0.14 (SD 0.04)	0.15
	Trapezium	−0.01 (SD 0.07)	−0.07 (SD 0.07)	0.10
	T-test (MC1-Trap)	5.35×10^{-6}***	0.0002***	/

curvatures of the facets of the MC1 and trapezium were comparable along the dorsal-volar axis ($t = -1.5694$, $df = 9.9979$, $P = 0.15$) but significantly different along the radial-ulnar axis ($t = 6.2629$, $df = 8.0581$, $P = 0.0002$) (Table 1).

4. Discussion

It has been shown recently that OA should not only be considered as a disease affecting articular cartilage but as a global joint disorder involving multiple factors (Conconi et al., 2014; Halilaj et al., 2015). Nevertheless, articular degradations remain the principal outcome of this disabling condition, leading many researchers to hypothesize that peak intra-articular stress (Brandt et al., 2009; Fontana et al., 2007; Jackson et al., 2004) and morphological differences (Felson, 2000; North and Rutledge, 1983) are important causes of OA.

We designed a CT-based method to assess joint space in vivo and provided 3D representations of distance fields to assess the variations of proximity patterns in different physiological postures and during activities of daily living. This approach was originally introduced to assess articular surfaces interactions, contact areas and avoid the inherent problems linked with in vivo cartilage measurements (Anderst and Tashman, 2003; Marai et al., 2004). Several models based on this technique have been developed to evaluate the link between joint congruence, articular morphology and early OA pathomechanics (Conconi et al., 2014; Dourthe et al., 2016; Halilaj et al., 2014a, 2014b, 2015; Lalone et al., 2013; Su et al., 2014). However, to our knowledge, no study has yet compared the contact biomechanics of the TMC joint between healthy and late stage OA subjects.

We observed that in OA patients, there is a decrease in TMC joint space and an increase in articular and proximity areas compared to the healthy subjects across different tasks and positions. Such phenomenon might be the result of a joint protection mechanism, as an increased articular surface can potentially help to redistribute the increasing load resulting from the progressive decrease in joint space. Conversely, this outcome might also simply result from the bone remodeling mechanism initiated by this constant increase in intra-articular pressure. Further investigations should be performed in the future to clearly identify what are the exact causes of such morphological adaptations and whether they can be categorized as the outcome of a joint protection mechanism.

The higher standard deviation observed in the measurements of articular areas in the OA group can be explained by differences in OA progression between the six subjects (Eaton stage III and IV). Important morphological changes were found in the 3D geometry of the articular surfaces, from a saddle-shaped healthy joint to a condyloid structure in late stage OA. This follows the findings of Nortwick et al. (2013), who identified three different types of trapezium morphology related to the progression of OA. More specifically, they reported that Eaton stage II specimens were mainly saddle-shaped, while Eaton stage III and IV were either dish- or cirque-shaped. These morphological changes also resulted in a large articular area of the TMC joint in OA patients.

The minimal joint space reported in the OA group was significantly smaller in comparison with healthy subjects. This agrees with Halilaj et al. (2015) and confirms the occurrence of joint space narrowing reported in late stage OA patients (Eaton et al., 1984; Eaton and Glickel, 1987). The minimal joint space values reported in the healthy group (0.6–0.9 mm) were slightly lower than the findings of Halilaj et al. (2015), who found an average joint space of 1.0 mm in healthy women. We also observed a significant enlargement of proximity areas between healthy and arthritic subjects. Together with the significant joint space narrowing observed, our findings suggest that the proximity between the MC1 and trapezium is increasing when OA is progressing, which agrees with previous reports in subjects with early to late stage OA

(stages I–IV) (Halilaj et al., 2014b, 2015; Xu et al., 1998). We observed a slight difference in the proximity areas calculated for the MC1 and trapezium in both groups. This can be explained by the automatic, non-uniform meshing, which creates triangles of different sizes to connect the vertices of each 3D bone model, leading to numerical differences between the proximity areas of the MC1 and trapezium.

Different proximity patterns were identified in the healthy population. The dominant pattern observed during abduction agrees with Halilaj et al. (2015) and Goto et al. (2014), who respectively located the contact area on the volar-radial and volar-central aspects of the TMC joint. During thumb abduction, Ateshian et al. (1995) located the contact area on the volar-ulnar aspect of the joint, which only agrees with our findings for the trapezium for the same configuration. The dominant pattern observed during thumb adduction (i.e. volar-central for the MC1 and volar-radial for the trapezium) agrees with Halilaj et al. (2015), but only for the trapezium. Our findings during thumb extension disagree with Ateshian et al. (1995), but agree with Halilaj et al. (2015), who reported the volar-central aspect of the MC1 and the dorsal-radial aspect of the trapezium as the locations of joint space centroids in this configuration. During flexion, the proximity area of the trapezium corresponds to the findings of Ateshian et al. (1995), who also located the contact area of the trapezium around its volar-ulnar aspect in this configuration. None of our findings during abduction-adduction and extension-flexion agree with Su et al. (2014), except for the dorsal-radial aspect of the trapezium that was also found in the extension posture. The dominant patterns observed in the neutral configuration (i.e. volar-central and -radial and central-radial) are consistent with the findings of Halilaj et al. (2015) and Ateshian et al. (1995). The dominant proximity patterns observed during lateral pinch (i.e. volar-central and volar-ulnar) agree with previous reports (Ateshian et al., 1995; Goto et al., 2014; Kuo et al., 2014). Finally, our observations in the neutral, lateral key pinch, and power grasp configurations agree with our previous findings (Dourthe et al., 2016).

Comparing our findings with the literature remains challenging due to the differences in methodologies, configurations studied, experimental setups and type of investigation (in vitro or in vivo). However, the most recurrent proximity patterns reported in our study are in agreement with previous findings (Koff et al., 2003; Pellegrini et al., 1993). In addition, our results reporting the volar and dorsal-radial aspect of the trapezium as recurrent regions of close proximity agree with Momose (1994) and Nortwick et al. (2013).

Previous in vitro investigations reported that the dorsal-radial aspect of the trapezium was the most affected by articular degradations (Kovler et al., 2004; Nortwick et al., 2013; Nufer et al., 2008), which we also identified as one of the dominant proximity patterns. Moreover, Xu et al. (1998) observed that the least affected region of the trapezium was the dorsal-ulnar aspect, which we reported as the least recurrent pattern.

We also investigated the displacements of proximity patterns between thumb postures. From abduction to adduction ('thumb adduction') and neutral to lateral key pinch, the proximity pattern of the MC1 shifted from radial to volar-ulnar, but no shift was reported for the trapezium. Between extension and flexion ('thumb flexion'), no shift was found for the MC1, but the proximity pattern of the trapezium moved from dorsal-radial to volar-ulnar. These displacements indicate that the contact area is moving between thumb postures, which might prevent that some specific articular sub-regions are under constant stress.

Conversely, the volar-central aspect of the MC1 was reported in the proximity patterns of every configuration besides the power grasp, which might indicate that the palmar beak of the MC1 is under constant high pressure in most thumb configurations. Such findings are in agreement with previous reports (Dourthe et al., 2016; Kovler et al., 2004; Pellegrini et al., 1993; Pelligrini, 1991b) and might explain the important deformations observed on this specific articular facet of the MC1 in the OA group (Fig. 6B).

The morphological comparison between healthy and OA subjects showed an inversion of the curvature of the proximal facet of the MC1 (concave to convex) and a flattening of the convex curvature of the distal facet of the trapezium along the dorsal-volar axis. These articular deformations result in a condylar shape of the TMC joint which might explain the altered thumb motions observed during the clinical examination of late stage OA patients (D'Agostino et al., 2017). Thumb flexion is usually preserved in these patients, which could be linked to the bulged and lengthened articular surface of the MC1 which runs inside the deepened articular surface of the trapezium (groove form). The impaired thumb abduction and axial rotation in OA patients could be explained by the deepening of the trapezium and the lengthening of its ulnar and radial horns. Together with the dorso-radial subluxation of the base of the MC1 (Fig. 6B), this leads to the adductus deformity of the thumb observed in patients with advanced TMC OA (stage III or IV).

We also observed that the proximity patterns of the MC1 and trapezium were not always mirrored, especially in adduction, flexion and lateral key pinch. This might suggest that during these specific tasks, the MC1 is shifting along the articular surface of the trapezium. Pelligrini (1991b) suggested that cartilage degradation was caused by shear forces generated by a translation of the MC1 on the trapezium. Based on this assumption, our findings indicate that early degradations of the articular cartilage may occur along a line connecting the centroids of the different proximity patterns observed between thumb postures.

The major advantage of this method is its applicability in vivo and its potential use in a clinical context. The main limitation of this study is that the calculations are based on 3D reconstructions of two-dimensional CT-images. Thus, the accuracy of the results mainly depends on scanning resolution and segmentation error. Previous research has shown that the segmentation error is in the order of 0.16–0.55 mm (Kerkhof et al., 2016; Lalone et al., 2015; Van den Broeck et al., 2014). This should be taken into account when interpreting the estimates of joint space, especially in the OA group, where the average minimal joint space is below the actual accuracy of the method. Another limitation of this study is the small size of the OA group, which does not allow any statistically relevant conclusion. However, the similarities observed between OA subjects still indicate a certain pattern that can provide further insights regarding the evolution of the disease. Finally, it remains important to note that proximity patterns are sensitive to the amplitude of the intra-articular contact forces, which can differ between tasks (Goislard de Monsabert et al., 2014). Indeed, a task requiring more strength (e.g. power grasp) might lead to an increased level of joint loading compared to a less demanding task (e.g. lateral key pinch), which can have an impact on the size of the corresponding proximity area. However, in this study, the difference between submaximal force amplitudes was not significant. This kind of phenomenon should be taken into account when interpreting the results regarding the potential correlation between contact geometry and hand posture.

5. Conclusions

Distinct proximity patterns were observed across tasks with a recurrent dominant pattern reported on the volar aspect of the MC1. The comparison between healthy and arthritic subjects showed a significant enlargement of the articular and proximity areas, in parallel with a significant joint space narrowing in TMC joints affects by OA. We also observed important articular deformations characterized by a transformation from saddle-shaped to condylar shape in late stage OA subject. Such insights can contribute to our understanding of the biomechanical behavior of the TMC joint and will ultimately lead to a better knowledge of the occurrence mechanisms of TMC OA.

Conflict of interests

This study was supported by the Materialise-Kulak Chair for Hand Surgery granted to EEV and FS by the company Materialise (Leuven, Belgium).

Acknowledgements

The authors would like to thank the two anonymous reviewers for their valuable comments on the original manuscript. We also thank the Orthopaedic Bioengineering Laboratories from Brown University (Providence RI, USA) for sharing the design of the custom-designed polycarbonate rig. In addition, we thank radiologist Dr. Eddy Brugman and the technical staff the Medical Imaging department of the AZ Groeninge (Kortrijk, Belgium) for their contribution to this study.

References

Anderst, W.J., Tashman, S., 2003. A method to estimate in vivo dynamic articular surface interaction. J. Biomech. 36, 1291–1299. http://dx.doi.org/10.1016/S0021-9290(03)00157-X.

Ateshian, G.A., Rosenwasser, M.P., Mow, V.C., 1992. Curvature characteristics and congruence of the thumb carpometacarpal joint: differences between female and male joints. J. Biomech. 25, 591–595. http://dx.doi.org/10.1016/0021-9290(92)90102-7.

Ateshian, G.A., Ark, J.W., Rosenwasser, M.P., Pawluk, R.J., Soslowsky, L.J., Mow, V.C., 1995. Contact areas in the thumb carpometacarpal joint. J. Orthop. Res. 13, 450–458. http://dx.doi.org/10.1002/jor.1100130320.

Batra, S., Kanvinde, R., 2007. Osteoarthritis of the thumb trapeziometacarpal joint. Curr. Orthop. 21, 135–144. http://dx.doi.org/10.1016/j.cuor.2007.02.006.

Brandt, K.D., Dieppe, P., Radin, E., 2009. Etiopathogenesis of osteoarthritis. Med. Clin. North Am. 93, 1–24. http://dx.doi.org/10.1016/j.mcna.2008.08.009.

Cheema, T., Salas, C., Morrell, N., Lansing, L., Reda Taha, M.M., Mercer, D., 2012. Opening wedge trapezial osteotomy as possible treatment for early trapeziometacarpal osteoarthritis: a biomechanical investigation of radial subluxation, contact area, and contact pressure. J. Hand. Surg. [Am.] 37, 699–705. http://dx.doi.org/10.1016/j.jhsa.2012.01.013.

Conconi, M., Halilaj, E., Parenti Castelli, V., Crisco, J.J., 2014. Is early osteoarthritis associated with differences in joint congruence? J. Biomech. 47, 3787–3793. http://dx.doi.org/10.1016/j.jbiomech.2014.10.030.

Crisco, J.J., Halilaj, E., Moore, D.C., Patel, T., Weiss, A.P.C., Ladd, A.L., 2015a. In vivo kinematics of the trapeziometacarpal joint during thumb extension-flexion and abduction-adduction. J. Hand. Surg. [Am.] 40, 289–296. http://dx.doi.org/10.1016/j.jhsa.2014.10.062.

Crisco, J.J., Patel, T., Halilaj, E., Moore, D.C., 2015b. The envelope of physiological motion of the first carpometacarpal joint. J. Biomech. Eng. 137, 101002. http://dx.doi.org/10.1115/1.4031117.

D'Agostino, P., Dourthe, B., Kerkhof, F., Vereecke, E.E., Stockmans, F., 2017. Impact of osteoarthritis and total joint arthroplasty on the kinematics of the trapeziometacarpal joint. J. Hand. Surg. [Am.] (under revision).

Dourthe, B., D'Agostino, P., Stockmans, F., Kerkhof, F., Vereecke, E., 2016. In vivo contact biomechanics in the trapeziometacarpal joint using finite deformation biphasic theory and mathematical modelling. Med. Eng. Phys. 38, 108–114. http://dx.doi.org/10.1016/j.medengphy.2015.11.003.

Eaton, R.G., Glickel, S.Z., 1987. Trapeziometacarpal osteoarthritis. Staging as a rationale for treatment. Hand Clin. 3, 455–471.

Eaton, R., Lane, L., Littler, J., K, J.J., 1984. Ligament reconstruction for the painful thumb carpometacarpal joint: a long-term assessment. J. Hand. Surg. [Am.] 9, 692–699.

Edmunds, J.O., 2011. Current concepts of the anatomy of the thumb trapeziometacarpal joint. J. Hand. Surg. [Am.] 36, 170–182. http://dx.doi.org/10.1016/j.jhsa.2010.10.029.

Felson, D.T., 2000. Osteoarthritis: new insights. Part 1: the disease and its risk factors. Ann. Intern. Med. 133, 635–646. http://dx.doi.org/10.7326/0003-4819-133-8-200010170-00016.

Fontana, L., Neel, S., Claise, J.M., Ughetto, S., Catilina, P., 2007. Osteoarthritis of the thumb carpometacarpal joint in women and occupational risk factors: a case-control study. J. Hand. Surg. [Am.] 32, 459–465. http://dx.doi.org/10.1016/j.jhsa.2007.01.014.

Goislard de Monsabert, B., Vigouroux, L., Bendahan, D., Berton, E., 2014. Quantification of finger joint loadings using musculoskeletal modelling clarifies mechanical risk factors of hand osteoarthritis. Med. Eng. Phys. 36, 177–184. http://dx.doi.org/10.1016/j.medengphy.2013.10.007.

Goto, A., Leng, S., Sugamoto, K., Cooney, W.P., Kakar, S., Zhao, K., 2014. In vivo pilot study evaluating the thumb carpometacarpal joint during circumduction. In: Clinical Orthopaedics and Related Research, pp. 1106–1113. http://dx.doi.org/10.1007/s11999-013-3066-8.

Halilaj, E., Laidlaw, D.H., Moore, D.C., Crisco, J.J., 2014a. Polar histograms of curvature for quantifying skeletal joint shape and congruence. J. Biomech. Eng. 136, 94503. http://dx.doi.org/10.1115/1.4027938.

Halilaj, E., Moore, D.C., Laidlaw, D.H., Got, C.J., Weiss, A.P.C., Ladd, A.L., Crisco, J.J., 2014b. The morphology of the thumb carpometacarpal joint does not differ between men and women, but changes with aging and early osteoarthritis. J. Biomech. 47, 2709–2714. http://dx.doi.org/10.1016/j.jbiomech.2014.05.005.

Halilaj, E., Rainbow, M.J., Got, C., Schwartz, J.B., Moore, D.C., Weiss, A.P.C., Ladd, A.L., Crisco, J.J., 2014c. In vivo kinematics of the thumb carpometacarpal joint during three isometric functional tasks. Clin. Orthop. Relat. Res. 472, 1114–1122. http://dx.doi.org/10.1007/s11999-013-3063-y.

Halilaj, E., Moore, D.C., Patel, T.K., Laidlaw, D.H., Ladd, A.L., Weiss, A.P.C., Crisco, J.J., 2015. Older asymptomatic women exhibit patterns of thumb carpometacarpal joint space narrowing that precede changes associated with early osteoarthritis. J. Biomech. 48, 3643–3649. http://dx.doi.org/10.1016/j.jbiomech.2015.08.010.

Hunter, D.J., Wilson, D.R., 2009. Role of alignment and biomechanics in osteoarthritis and implications for imaging. Radiol. Clin. N. Am. 47, 553–566. http://dx.doi.org/10.1016/j.rcl.2009.04.006.

Jackson, B.D., Wluka, A.E., Teichtahl, A.J., Morris, M.E., Cicuttini, F.M., 2004. Reviewing knee osteoarthritis - a biomechanical perspective. J. Sci. Med. Sport 7, 347–357. http://dx.doi.org/10.1016/S1440-2440(04)80030-6.

Kerkhof, F.D., Brugman, E., D'Agostino, P., Dourthe, B., van Lenthe, G.H., Stockmans, F., Jonkers, I., Vereecke, E.E., 2016. Quantifying thumb opposition kinematics using dynamic computed tomography. J. Biomech. 49, 1994–1999. http://dx.doi.org/10.1016/j.jbiomech.2016.05.008.

Koff, M.F., Ugwonali, O.F., Strauch, R.J., Rosenwasser, M.P., Ateshian, G.A., Mow, V.C., 2003. Sequential wear patterns of the articular cartilage of the thumb carpometacarpal joint in osteoarthritis. J. Hand. Surg. [Am.] 28, 597–604. http://dx.doi.org/10.1016/S0363-5023(03)00145-X.

Kovler, M., Lundon, K., McKee, N., Agur, A., 2004. The human first carpometacarpal joint: osteoarthritic degeneration and 3-dimensional modeling. J. Hand Ther. 17, 393–400. http://dx.doi.org/10.1197/j.jht.2004.07.001.

Kuo, L.-C., Lin, C.-J., Chen, G.-P., Jou, I.-M., Wang, C.-K., Goryacheva, I.G., Dosaev, M.Z., Su, F.-C., 2014. In vivo analysis of trapeziometacarpal joint kinematics during pinch tasks. Biomed. Res. Int. 2014, 1–8. http://dx.doi.org/10.1155/2014/157295.

Lalone, E.A., McDonald, C.P., Ferreira, L.M., Peters, T.M., King, G.W., Johnson, J.A., 2013. Development of an image-based technique to examine joint congruency at the elbow. Comput. Methods Biomech. Biomed. Engin. 16, 280–290. http://dx.doi.org/10.1080/10255842.2011.617006.

Lalone, E.A., Willing, R.T., Shannon, H.L., King, G.J.W., Johnson, J.A., 2015. Accuracy assessment of 3D bone reconstructions using CT: an intro comparison. Med. Eng. Phys. 37, 729–738. http://dx.doi.org/10.1016/j.medengphy.2015.04.010.

Luker, K.R., Aguinaldo, A., Kenney, D., Cahill-Rowley, K., Ladd, A.L., 2014. Functional task kinematics of the thumb carpometacarpal joint. In: Clinical orthopaedics and Related Research, pp. 1123–1129. http://dx.doi.org/10.1007/s11999-013-2964-0.

Marai, G.E., Laidlaw, D.H., Demiralp, Ç., Andrews, S., Grimm, C.M., Crisco, J.J., 2004. Estimating joint contact areas and ligament lengths from bone kinematics and surfaces. IEEE Trans. Biomed. Eng. 51, 790–799. http://dx.doi.org/10.1109/TBME.2004.826606.

Momose, T., 1994. Cartilage degeneration and measurement of the contact area of the trapeziometacarpal joint: morphological observation. Nippon Seikeigeka Gakkai Zasshi 68, 426–434.

Momose, T., Nakatsuchi, Y., Saitoh, S., 1999. Contact area of the trapeziometacarpal joint. J. Hand. Surg. [Am.] 24, 491–495. http://dx.doi.org/10.1053/jhsu.1999.0491.

Moulton, M.J., Parentis, M.A., Kelly, M.J., Jacobs, C., Naidu, S.H., Pellegrini, V.D., 2001. Influence of metacarpophalangeal joint position on basal joint-loading in the thumb. J. Bone Joint Surg. Am. 83–A, 709–716.

Neumann, D.A., Bielefeld, T., 2003. The carpometacarpal joint of the thumb. J. Orthop. Sports Phys. Ther. 33, 246–251. http://dx.doi.org/10.2519/jospt.2003.33.7.386.

Nicholas, R.M., Calderwood, J.W., 1992. De la Caffinière arthroplasty for basal thumb joint osteoarthritis. J. Bone Joint Surg. (Br.) 74, 2–5.

North, E.R., Rutledge, W.M., 1983. The trapezium-thumb metacarpal joint: the relationship of joint shape and degenerative joint disease. Hand 15, 201–206. http://dx.doi.org/10.1016/S0072-968X(83)80014-X.

Nortwick, S. Van, Berger, A., Cheng, R., Lee, J., Ladd, A.L., 2013. Trapezial topography in thumb carpometacarpal arthritis. J. Wrist Surg. 2, 263–270. http://dx.doi.org/10.1055/s-0033-1350088.

Nufer, P., Goldhahn, J., Kohler, T., Kuhn, V., Müller, R., Herren, D.B., 2008. Microstructural adaptation in trapezial bone due to subluxation of the thumb. J. Orthop. Res. 26, 208–216. http://dx.doi.org/10.1002/jor.20500.

Pellegrini, V.D., Olcott, C.W., Hollenberg, G., 1993. Contact patterns in the trapeziometacarpal joint: the role of the palmar beak ligament. J. Hand. Surg. [Am.] 18, 238–244. http://dx.doi.org/10.1016/0363-5023(93)90354-6.

Pelligrini, V.D., 1991a. Osteoarthritis of the trapeziometacarpal joint: the pathophysiology of articular cartilage degeneration. II. Articular wear patterns in the osteoarthritic joint. J. Hand. Surg. [Am.] 16, 975–982. http://dx.doi.org/10.1016/S0363-5023(10)80055-3.

Pelligrini, V.D., 1991b. Osteoarthritis of the trapeziometacarpal joint: the pathophysiology of articular cartilage degeneration. I. Anatomy and pathology of the aging joint. J. Hand. Surg. [Am.] 16, 967–974. http://dx.doi.org/10.1016/S0363-5023(10)80055-3.

R Core Team, 2013. R: A language and environment for statistical computing. R Found. Stat. Comput., Vienna, Austria3-900051-07-0(URL http//www.R-project.org/).

Su, F.-C.C., Lin, C.-J.J., Wang, C.-K.K., Chen, G.-P.P., Sun, Y.-N.N., Chuang, A.K., Kuo, L.-C.C., 2014. In vivo analysis of trapeziometacarpal joint arthrokinematics during multi-directional thumb motions. Clin. Biomech. 29, 1009–1015. http://dx.doi.org/10.1016/j.clinbiomech.2014.08.012.

Tsai, P., Beredjiklian, P.K., 2008. Physical diagnosis and radiographic examination of the thumb. Hand Clin. 24, 231–237. http://dx.doi.org/10.1016/j.hcl.2008.03.004.

Van den Broeck, J., Vereecke, E., Wirix-Speetjens, R., Vander Sloten, J., 2014. Segmentation accuracy of long bones. Med. Eng. Phys. 36, 949–953. http://dx.doi.

org/10.1016/j.medengphy.2014.03.016.
Wilder, F.V., Barrett, J.P., Farina, E.J., 2006. Joint-specific prevalence of osteoarthritis of the hand. Osteoarthr. Cartil. 14, 953–957. http://dx.doi.org/10.1016/j.joca.2006.04.013.
Wilson, D.R., McWalter, E.J., Johnston, J.D., 2008. The measurement of joint mechanics and their role in osteoarthritis genesis and progression. Rheum. Dis. Clin. N. Am. 34, 605–622. http://dx.doi.org/10.1016/j.rdc.2008.05.002.
Wilson, D.R., McWalter, E.J., Johnston, J.D., 2013. The measurement of joint mechanics and their role in osteoarthritis genesis and progression. Rheum. Dis. Clin. N. Am. 39, 21–44. http://dx.doi.org/10.1016/j.rdc.2012.11.002.
Xu, L., Strauch, R.J., Ateshian, G.A., Pawluk, R.J., Mow, V.C., Rosenwasser, M.P., 1998. Topography of the osteoarthritic thumb carpometacarpal joint and its variations with regard to gender, age, site, and osteoarthritic stage. J. Hand. Surg. [Am.] 23, 454–464. http://dx.doi.org/10.1016/S0363-5023(05)80463-0.